Study of plasmon resonance in Bi$_2$Se$_3$ and Sb$_2$Te$_3$ by infrared spectral ellipsometry

© E.H. Alizade

Institute of Physics, National Academy of Sciences of Azerbaijan,
AZ1141 Baku, Azerbaijan

e-mail: AlizadeElv@gmail.com

In the infrared region of the spectrum (IR), the optical properties of single-crystal samples of narrow-gap degenerate semiconductors Bi$_2$Se$_3$ and Sb$_2$Te$_3$ are investigated by infrared spectral ellipsometry (SE). The transport properties of the Drude fitting of dielectric functions obtained by spectroscopic ellipsometry are studied. The behavior of the bulk and surface plasmon polaritons is investigated in detail. The dispersion and mean free path of the plasmon, the depth of the skin layer for the conducting and dielectric surfaces are calculated. The contribution of the plasmon to the optical properties is estimated from the spectral density for the Bi$_2$Se$_3$ and Sb$_2$Te$_3$ samples.

Keywords: ellipsometry, plasmon, plasmonics, plasmon dispersion, plasmon mean free path, plasmon penetration depth.

Introduction

The incident electromagnetic wave on the surface of the metal-dielectric interface is able to excite collective oscillations of free charge carriers. These oscillations are either volumetric (VPP) or surface (SPP) plasmon-polaritons [1]. Recently, surface plasmon resonance (SPR) [2–6] has attracted considerable researchers' interest. Most of the studies in this topic are devoted to observation of SPR in noble metals (gold, silver, etc., etc.) and indium-tin oxide. This is a very convenient and sensitive tool for detection and analysis of the compounds composition.

Narrow-bandgap degenerate semiconductors are promising for use in IR plasmonics, since they have a plasmon resonance in the mid-IR range. This effect is studied within the scope of this article and will be shown using the example of Bi$_2$Se$_3$ and Sb$_2$Te$_3$. Previously, it was shown in the literature that the SPR excitation frequencies in Bi$_2$Se$_3$ and Sb$_2$Te$_3$ fall in the IR region, thereby studying Bi$_2$Se$_3$ and Sb$_2$Te$_3$ as plasmonic materials is becoming a very promising direction. The plasma frequency depends on the concentration of free charge carriers, this dependence is described by the well-known formula [7]:

$$\omega_p = \sqrt{\frac{Ne^2}{m^* \varepsilon_0 \varepsilon_\infty}},$$

where N — carrier concentration, e — electron charge, m^* — effective free charge carrier mass, ε_0 — vacuum dielectric constant and ε_∞ — high-frequency dielectric constant. Thus, it is possible to shift the maximum SPR frequency in a wide region of the IR spectrum by changing the charge carriers concentration by changing the stoichiometry of the conducting compounds. This is an important advantage over noble metals.

The SPR sensor has a dielectric/conductor/dielectric design, one of the dielectrics in which is the ligand layer. The ligand layer is responsible for selective binding to detectable molecules. Since the lattice vibrational modes for most compounds are observed in the IR region, the SPR sensor will be most sensitive when operating in the IR spectrum. For a dielectric/metal/dielectric optical system, the position of the reflection minimum at surface plasmon resonance will depend on the dielectric constant of the external medium [8]. Thus, by selecting an appropriate ligand layer on the surface of a conducting compound thin film, selective optical detection of various compounds is implemented due to plasmon resonance. Detection occurs due to a shift of the position of the reflection minimum during SPR, or due to a shift of the angle of the reflection minimum when the external medium dielectric constant changes.

SPP excitation is possible under condition of equality $k_x = k_{spp}$, where k_x — projection of the wave number of the exciting electromagnetic wave and k_{spp} — SPP wave number. The wave number of an exciting electromagnetic wave is always less than the wave number of the SPP k_{spp}. For this, prismatic input methods (Kretschmann scheme) or diffraction on the diffractor grating surface are used. The projection of the wave number of an electromagnetic wave for the case of the Kretschmann scheme is [8]

$$k_x = \frac{\omega}{c} \sqrt{\varepsilon_a} \sin(\theta), \qquad (1)$$

where ω — frequency of the electromagnetic wave, ε_a — prism dielectric constant, c — speed of light and θ — wave incidence angle.
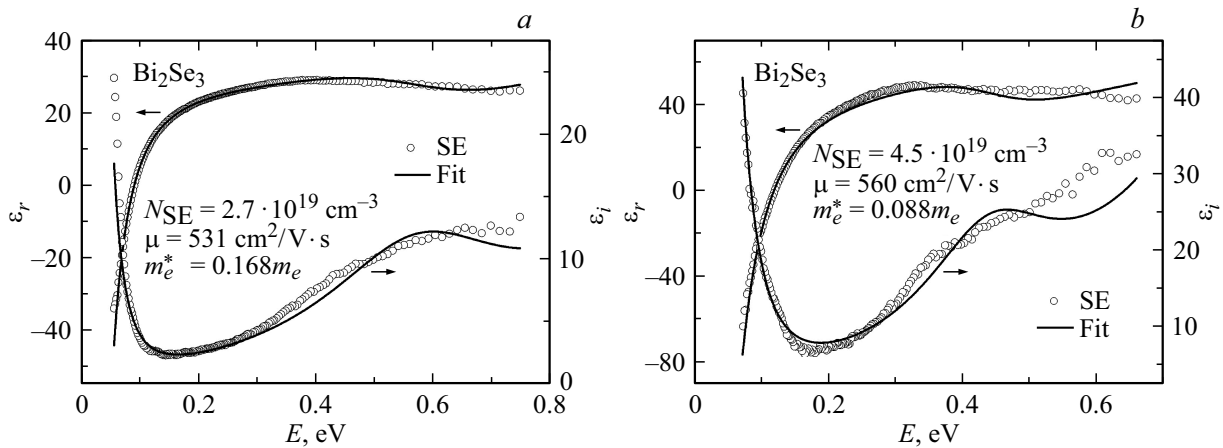
Figure 1. Experimental and fitting dielectric function (*a*) Bi_2Se_3 and (*b*) Sb_2Te_3, ε_r is a real part and ε_i is an imaginary part of dielectric function.

Previously, articles on plasmon observation in these compounds and in other structures of the tetradymite [7,9,10] type were published, but there is no information in the literature about SPR and its application for IR plasmon devices and the study of plasmon properties. In this work, this is done for the first time.

Experiment details

Bi_2Se_3 and Sb_2Te_3 single-crystal samples were obtained by the Bridgeman−Stockbarger method. Details of the processing method, a detailed description of the structure, X-ray diffraction and Raman spectroscopy for the samples used are described in the articles [7,11]. The compounds obtained are classified as crystalline materials with space group $R\bar{3}m$.

The concentration of charge carriers was determined based on measurements of the Hall effect. The Hall effect was measured by the standard four-probe method in a constant magnetic field of 1.5 T. The measured samples were in the form of a parallelepiped with dimensions $2.3 \times 0.5 \times 10$ mm, $2.1 \times 0.3 \times 9$ mm. Electrical contacts were applied with indium. The measuring current through the sample was 50 mA. Hall effect measurements were carried out with two directions of the magnetic field and two directions of the measuring current in order to eliminate spurious signals.

Ellipsometric studies were carried out at room temperature using a J.A. Woollam IR-VASE ellipsometer [7]. The measurements were carried out within the photon energy range from 0.035 to 0.6 eV in air. Samples delaminated from bulk ingots with perpendicular orientation with respect to the optical axis and with a mirror surface were studied. The plane of IR light incidence is perpendicular to the surfaces. Dielectric capacity ($\varepsilon = \varepsilon_r + i\varepsilon_i$), extracted using the ellipsometric parameters Ψ and Δ, did not depend on the angle, therefore, it corresponded to the component $E \perp C$

(E — electric vector of the incident light, C — optical axis) of the dielectric function tensor.

Results

As noted above, the SPR frequency depends on the concentration and effective mass of charge carriers. The charge carrier concentration obtained from the Hall effect on Bi_2Se_3 and Sb_2Te_3 is equal to $n = 2.9 \cdot 10^{19}$ cm^{-3} and $p = 4.5 \cdot 10^{19}$ cm^{-3} respectively. Thus, with the help of these data, the transport parameters were estimated with the maximum approximation by the optical method, i.e., from ellipsometric measurements. The spectral dependence of the dielectric function on the photon energy associated with the presence of free charge carriers is described by the Drude oscillator [12]:

$$\varepsilon_{\text{Drude}}(E) = \frac{-\hbar^2 e^2 N \mu}{\varepsilon_0(\mu m_{e(h)}^* E^2 + ie\hbar E)}.$$

Here, the charge carrier concentration N, the mobility μ, and the effective mass $m_{e(h)}^*$ are fitting parameters. To take into account interband transitions, the Lorentz oscillator was used:

$$\varepsilon_{\text{Lorenz}}(E) = \frac{A\Gamma E_C}{E_C^2 - E^2 - iE\Gamma},$$

where A — oscillator amplitude, Γ — broadening, and E_C — transition energy. Thus, compound dispersion was described by the expression $\varepsilon(E) = \varepsilon_{\text{Drude}}(E) + \varepsilon_{\text{Lorenz}}(E)$.

The experimental (SE) and fitting (Fit) dielectric functions for both compounds are given in Fig. 1. The fitting was performed using the Levenberg−Marquardt optimization method. As can be seen from Fig. 1, fitting describes well the experimental data with mean square errors of 7 and 13 for Bi_2Se_3 and Sb_2Te_3, respectively. In spectroscopic ellipsometry, it's generally accepted that fitting is reliable if the root mean square error does not exceed 20.
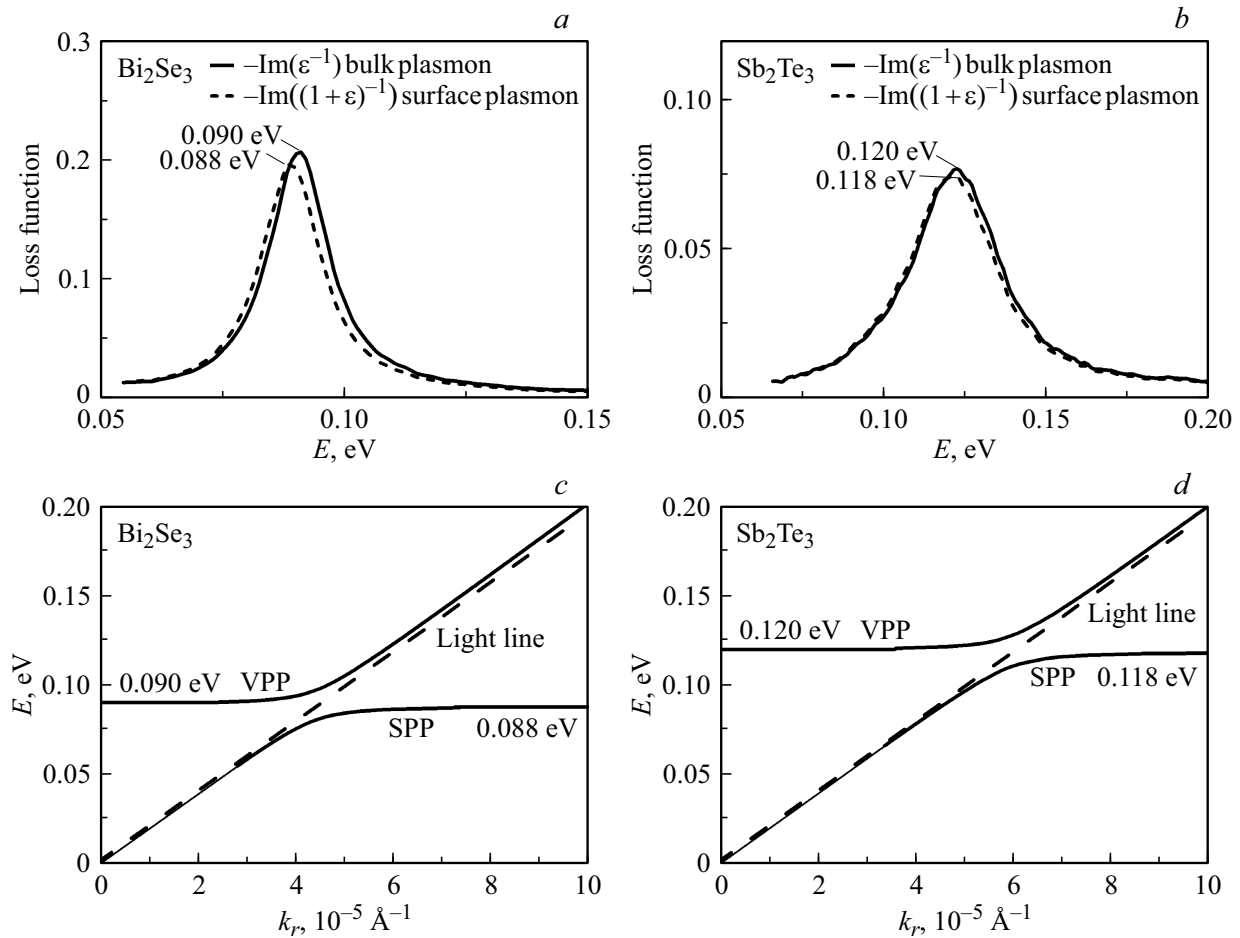
Figure 2. Loss function of surface (dashed line) and volume (solid line) plasmons (*a*) Bi$_2$Se$_3$ and (*b*) Sb$_2$Te$_3$. Dispersion of volumetric (VPP) and surface (SPP) plasmons for Bi$_2$Se$_3$ (*c*) and Sb$_2$Te$_3$ (*d*), dashed line — light line.
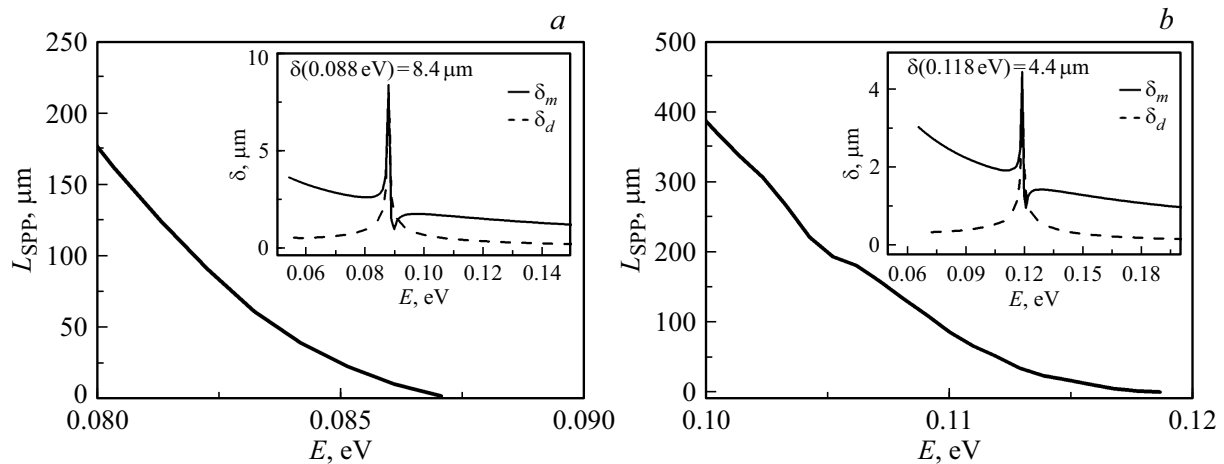
Figure 3. Surface plasmon mean free path length for (*a*) Bi$_2$Se$_3$ and (*b*) Sb$_2$Te$_3$. In the insertion, the penetration depth of plasmon excitation into the conductor (solid line) and dielectric (dashed line).

The concentrations of charge carriers were determined based on the fitting results and compared with the Hall effect data. It turned out for Bi$_2$Se$_3$ $N_{SE} = 2.7 \cdot 10^{19}\,\mathrm{cm}^{-3}$ and $N_H = 2.9 \cdot 10^{19}\,\mathrm{cm}^{-3}$, and for Sb$_2Te_3$ $N_{SE} = 4.5 \cdot 10^{19}\,\mathrm{cm}^{-3}$ and $N_H = 4.5 \cdot 10^{19}\,\mathrm{cm}^{-3}$, respectively. Good agreement can be seen between the obtained concentrations for both compounds. The effective masses obtained from fitting are $0.16 m_e$ and $0.08 m_e$ for

Bi_2Se_3 and Sb_2Te_3, respectively. These data are in full agreement with those given in the literature [13] $0.16m_e$ for Bi_2Se_3, while for Sb_2Te_3 the values differ, and the study of this difference nature requires a separate analysis, which is not within the scope of this article. The mechanism of change in effective masses was previously studied on the example of silicon in [14]. The change occurs due to the contribution of valleys in the band structure with heavier carriers, whose contribution to the carrier concentration increases with concentration increase. The mechanism may be similar to those observed in Bi_2Se_3 and Sb_2Te_3. However, an accurate statement requires an additional study of samples with different carrier concentrations.

The charge carrier concentration and the effective mass have a direct effect on the plasmon resonance spectrum. The plasmon resonance energy is determined based on the loss function, $-\mathrm{Im}(\varepsilon^{-1})$ and $-\mathrm{Im}((1+\varepsilon)^{-1})$ for volumetric and surface plasmons, respectively [15]. At the resonant frequency, the loss of the optical signal increases, on the loss functions (Fig. 1, a) for Bi_2Se_3 and (Fig. 1, b) for Sb_2Te_3, the exact value of the plasmon resonance energy is determined based on the peak position. The volumetric plasmon resonance energy is $0.090\,\mathrm{eV}$ and $0.120\,\mathrm{eV}$ for Bi_2Se_3 and Sb_2Te_3, respectively, while for SPR it is expected to be lower than — $0.088\,\mathrm{eV}$ and $0.118\,\mathrm{eV}$ for Bi_2Se_3 and Sb_2Te_3, respectively.

Figure 2, c, d shows the dispersion diagrams of volumetric (VPP) and surface (SPP) plasmons for Bi_2Se_3 and Sb_2Te_3, calculated based on the real part of the wave vector by the formula [16]:

$$k = k_1 + ik_2 = \left[\frac{\omega}{c}\left(\frac{\varepsilon_r \varepsilon_a}{\varepsilon_r + \varepsilon_a}\right)^{1/2}\right] + i\left[\frac{\omega}{c}\left(\frac{\varepsilon_r \varepsilon_a}{\varepsilon_r + \varepsilon_a}\right)^{3/2}\frac{\varepsilon_i}{2(\varepsilon_r)^2}\right].$$

The imaginary part k_2 characterizes propagation of plasmon excitation along the dielectric/conductor interface, the mean free path length is $L_{spp} = \frac{1}{2k_2}$ (Fig. 3). The mean free path length corresponds to the distance at which plasmon excitation attenuates by e times. This parameter makes it possible to characterize surface plasmon propagation.

The insertions to Fig. 3 show calculations of the penetration depths of the plasmon resonance into the dielectric and conducting media. The penetration depth is obtained by the formula

$$\delta_d = \frac{c}{\omega}\left|\frac{\varepsilon_1 + \varepsilon_a}{\varepsilon_a^2}\right|^{1/2}$$

for dielectric medium and

$$\delta_m = \frac{c}{\omega}\left|\frac{\varepsilon_1 + \varepsilon_a}{\varepsilon_1^2}\right|^{1/2}$$

for conducting medium [16]. Both parameters at the resonance point were $8.4\,\mu\mathrm{m}$ and $4.4\,\mu\mathrm{m}$ for Bi_2Se_3 and Sb_2Te_3, respectively. This parameter characterizes the depth at

which the plasmon attenuate by e times. Thus, it is possible to estimate to what depth plasmon is able „to probe" the external medium. This is an important parameter for creating selective detectors.

Conclusion

In this article, the properties of plasmon in Bi_2Se_3 and Sb_2Te_3 compounds are studied. The use of these degenerate narrow-bandgap semiconductors for IR plasmonics is shown to be promising. The effective masses of charge carriers are estimated. The spectral positions of the volumetric and surface plasmon polaritons are determined based on the loss function and calculated dispersions, and a difference between plasmon energies is observed that exceeds the measurement resolution. The free path parameters and the plasmon penetration depth are calculated.

References

[1] J.M. Pitarke, V.M. Silkin, E.V. Chulkov, P.M. Echenique. Rep. Prog. Phys., **70** (1), 1–87 (2006). DOI.org/10.1088/0034-4885/70/1/R01

[2] J. Gong, R. Dai, Z. Wang, Z. Zengming. Sci. Rep., **5**, 9279 (2015). DOI.org/10.1038/srep09279

[3] A. Melikyan, N. Lindenmann, S. Walheim, P. M. Leufke, S. Ulrich, J. Ye, P. Vincze, H. Hahn, Th. Schimmel, C. Koos, W. Freude, J. Leuthold. Opt. Express, **19** (9), 8855 (2011). DOI.org/10.1364/OE.19.008855

[4] A.N. Spitsyn, D.V. Utkin, O.S. Kuznetsov, P.S. Erokhin, N.A. Osina, V.I. Kochubey. Opt. i spektr., **129** (1), 100 (2021) (in Russian). DOI: 10.21883/OS.2021.01.50446.200-20

[5] A.V. Dyshlyuk, E.V. Mitsai, A.B. Cherepakhin, O.B. Vitrik, Yu.N. Kulchin. Pisma v ZHTF., **43** (15), 87 (2017) (in Russian). DOI: 10.21883/PJTF.2017.15.44875.16646

[6] A.V. Dyshlyuk, O.B. Vitrik, Guohui Lu, Yu.N. Kulchin. Pisma v ZHTF., **41** (12), 56 (2015) (in Russian).

[7] N.T. Mamedov, E.H. Alizade, Z.A. Jahangirli, Z.S. Aliev, N.A. Abdullayev, S.N. Mammadov, I.R. Amiraslanov, Yong-Gu Shim, Kazuki Wakita, S.S. Ragimov, A.I. Bayramov, Mahammad B. Babanly, A.M. Shikin, E.V. Chulkov. J. Vac. Sci. Technol. B, **37** (6), 062602 (2019). DOI: 10.1116/1.5122776

[8] S.A. Maier. *Plasmonics: Fundamentals and Applications,* 1st ed. (Springer, New York, 2007). https://DOI.org/10.1007/0-387-37825-1

[9] Z.S. Aliev, E.C. Ahmadov, D.M. Babanly, I.R. Amiraslanov, M.B. Babanly. Calphad, **66**, 101650 (2019). DOI: 10.1016/j.calphad.2019.101650

[10] P. Di Pietro, F.M. Vitucci, D. Nicoletti, L. Baldassarre, P. Calvani, R. Cava, Y.S. Hor, U. Schade, S. Lupi. Phys. Rev. B, **86**, 045439 (2012), DOI: 10.1103/PhysRevB.86.045439

[11] B.M. Goltzman, V.A. Kudinov, I.A. Smirnov. *Poluprovodnikovye termoelektricheskie materialy na osnove Bi_2Te_3* (Nauka, Moskva, 1972) (in Russian).

[12] T.E. Tiwald, D.W. Thompson, J.A.Woollam, W. Paulson, R. Hance. Thin Solid Films, **313–314**, 661–666 (1998). DOI.org/10.1016/S0040-6090(97)00973-5

[13] J. Heremans, R. Cava, N. Samarth. Nat. Rev. Mater., **2**, 17049 (2017). DOI.org/10.1038/natrevmats.2017.49

[14] M. Miyao, T. Motooka, N. Natsuaki, T. Tokuyama. Solid State Commun., **37** (7), 605-608 (1981). DOI.org/10.1016/0038-1098(81)90144-7

[15] G.L. Tan, L.K. DeNoyer, R.H. French, M.J. Guittet, M. Gautier-Soyer. J. Electron. Spectrosc. Relat. Phenom., **142** (2), 97–103 (2005). DOI.org/10.1016/j.elspec.2004.09.002

[16] William L. Barnes. J. Opt. A: Pure Appl. Opt., **8** (4), S87–S93 (2006). DOI.org/10.1088/1464-4258/8/4/S06